



## 2 On the spurious eigenvalues for a concentric sphere in BIEM

3 Jeng-Tzong Chen<sup>a,b,\*</sup>, Shing-Kai Kao<sup>a</sup>, Ying-Te Lee<sup>a</sup>, Yi-Jhou Lin<sup>a</sup>4 <sup>a</sup>Department of Harbor and River Engineering, National Taiwan Ocean University, Keelung 20224, Taiwan5 <sup>b</sup>Department of Mechanical and Mechanical Engineering, National Taiwan Ocean University, Keelung 20224, Taiwan

## 6 ARTICLE INFO

## 9 Article history:

10 Received 12 November 2008

11 Received in revised form 23 July 2009

12 Accepted 3 August 2009

13 Available online xxxx

## 14 Keywords:

15 Null-field integral equation

16 Degenerate kernel

17 Eigenproblem

18 Q1 Spurious eigenvalue

19 Singular value decomposition

## 2 A B S T R A C T

In this paper, the null-field integral equation method is employed to study the occurring mechanism of spurious eigenvalues for a concentric sphere. By expanding the fundamental solution into degenerate kernels and expressing the boundary density in terms of spherical harmonics, all boundary integrals can be analytically determined. It is noted that our null-field integral formulation can locate the collocation point on the real boundary thanks to the degenerate kernel. In addition, the spurious eigenvalues are parasitized in the formulations while true eigensolutions are dependent on the boundary condition such as the Dirichlet or Neumann problem. By using the updating term and updating document of singular value decomposition (SVD) technique, true and spurious eigenvalues can be extracted out, respectively. Besides, true and spurious boundary eigenvectors are obtained in the right and left unitary vectors in the SVD structure of the influence matrices. This finding agrees with that of 2D cases (Chen et al., in press [1]).

Crown Copyright © 2009 Published by Elsevier Ltd. All rights reserved.

35

## 36 1. Introduction

The application of eigenanalysis is gradually increasing for vibration and acoustics. The demand for eigenanalysis calls for an efficient and reliable method of computation for eigenvalues and eigenmodes. Over the past three decades, several boundary element formulations had been employed to solve the eigenproblems [2], e.g., determinant searching method, internal cell method, dual reciprocity method, particular integral method and multiple reciprocity method. In this paper, we will focus on the determinant searching method with emphasis on spurious eigenvalues when using the BIEM for 3D problems with an inner cavity. Spurious and fictitious solutions stem from the problems of non-uniqueness solution which appear in different aspects in computational mechanics. First of all, the occurrence of hourglass modes in the finite element method (FEM) using the reduced integration stems from the rank deficiency [3]. Also, loss of divergence-free constraint for the incompressible elasticity results in spurious modes. On the other hand, while solving the differential equation by using the finite difference method (FDM), the spurious eigenvalue also appears due to discretization [4–6]. In the real-part BEM [7] or the MRM formulation [8–13], spurious eigensolutions occur in

solving eigenproblems. Even though the complex-valued kernel is adopted, the spurious eigensolution also occurs for the multiply-connected problem [14,15] as well as the appearance of fictitious frequency for the exterior acoustics [16]. Spurious eigenvalues in the MFS for 3D problems were also studied by Tsai et al. [17]. In this paper, a simple case of 3D concentric sphere will be demonstrated to see how spurious eigensolutions occur and how they are suppressed by using singular value decomposition (SVD).

In the recent years, the SVD technique has been applied to solve problems of fictitious frequency [16] and continuum mechanics [18]. Two ideas, namely updating term and updating document [16], were successfully applied to extract the true and spurious solutions, respectively. In this paper, the three-dimensional eigenproblem of a concentric sphere is studied in both numerical and analytical ways. Owing to the introduction of degenerate kernel, the collocation point can be located exactly on the real boundary. Besides, true and spurious equations can be found by using the null-field integral equation in conjunction with degenerate kernels and spherical harmonics for a concentric sphere. Surface distributions of the inner and outer boundaries can be expanded in terms of spherical harmonics. Since a spurious eigenvalue is embedded in the numerical method and has no physical meaning, the remedies, SVD updating term and SVD updating document, are used to extract or filter out true and spurious eigenvalues, respectively. Finally, an example with various boundary conditions is utilized to validate the present approach by using singular and hypersingular formulations.

\* Corresponding author. Address: Department of Harbor and River Engineering, National Taiwan Ocean University, Keelung 20224, Taiwan. Tel.: +886 2 24622192x6177; fax: +886 2 24632375.

E-mail address: jtchen@mail.ntou.edu.tw (J.-T. Chen).

22  
23  
24  
25  
26  
27  
28  
29  
30  
31  
32  
33  
34  
58  
59  
60  
61  
62  
63  
64  
65  
66  
67  
68  
69  
70  
71  
72  
73  
74  
75  
76  
77  
78  
79  
80  
81  
82  
83  
84

## 85 2. Null-field integral equation formulation

### 86 2.1. Problem statements

87 The governing equation for the eigenproblem of a concentric  
88 sphere is the Helmholtz equation as follows:

$$90 (\nabla^2 + k^2)u(x) = 0, \quad x \in D, \quad (1)$$

91 where  $\nabla^2$ ,  $k$  and  $D$  are the Laplacian operator, the wave number  
92 and the domain of interest, respectively. The concentric sphere is  
93 depicted in Fig. 1. The inner and outer radii are  $a$  and  $b$ , respectively.

### 94 2.2. Dual null-field integral formulation—the conventional version

95 The dual boundary integral formulation [6] for the domain  
96 point is shown below:

$$99 4\pi u(x) = \int_B T(s, x)u(s)dB(s) - \int_B U(s, x)\frac{\partial u(s)}{\partial n_s}dB(s), \quad x \in D, \quad (2)$$

$$4\pi \frac{\partial u(x)}{\partial n_x} = \int_B M(s, x)u(s)dB(s) - \int_B L(s, x)\frac{\partial u(s)}{\partial n_s}dB(s), \quad x \in D, \quad (3)$$

100 where  $x$  and  $s$  are the field and source points, respectively,  $B$  is the  
101 boundary,  $n_x$  and  $n_s$  denote the outward normal vector at the field  
102 point and the source point, respectively, and the kernel function  
103  $U(s, x)$  is the fundamental solution which satisfies

$$105 (\nabla^2 + k^2)U(s, x) = 4\pi\delta(x - s), \quad (4)$$

106 where  $\delta$  is the Dirac-delta function. The other kernel functions can  
107 be obtained as

$$109 T(s, x) = \frac{\partial U(s, x)}{\partial n_s}, \quad (5)$$

$$L(s, x) = \frac{\partial U(s, x)}{\partial n_x}, \quad (6)$$

$$M(s, x) = \frac{\partial^2 U(s, x)}{\partial n_s \partial n_x}. \quad (7)$$

110 If the collocation point  $x$  is on the boundary, the dual boundary inte-  
111 gral equations for the boundary point can be obtained as follows:  
112

$$114 2\pi u(x) = C.P.V. \int_B T(s, x)u(s)dB(s) \\ - R.P.V. \int_B U(s, x)\frac{\partial u(s)}{\partial n_s}dB(s), \quad x \in B, \quad (8)$$

$$117 2\pi \frac{\partial u(x)}{\partial n_x} = H.P.V. \int_B M(s, x)u(s)dB(s) \\ - C.P.V. \int_B L(s, x)\frac{\partial u(s)}{\partial n_s}dB(s), \quad x \in B, \quad (9)$$

118 where  $R.P.V.$ ,  $C.P.V.$  and  $H.P.V.$  are the Riemann principal value,  
119 the Cauchy principal value and the Hadamard (or called Mangler) prin-

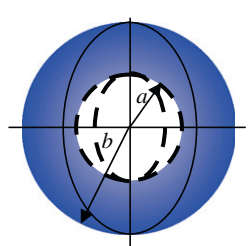


Fig. 1. A concentric sphere.

120 principal value, respectively. By collocating  $x$  outside the domain, we  
121 obtain the null-field integral equation as shown below:

$$122 0 = \int_B T(s, x)u(s)dB(s) - \int_B U(s, x)\frac{\partial u(s)}{\partial n_s}dB(s), \quad x \in D^c, \quad (10)$$

$$0 = \int_B M(s, x)u(s)dB(s) - \int_B L(s, x)\frac{\partial u(s)}{\partial n_s}dB(s), \quad x \in D^c, \quad (11)$$

125 where  $D^c$  denotes the complementary domain.

### 126 2.3. Dual null-field integral formulation—the present version

127 By introducing the degenerate kernels, the collocation points  
128 can be located on the real boundary free of facing the principal val-  
129 ue by using the bump contour approach. Therefore, the represen-  
130 tations of integral equations including the boundary point can be  
131 written as

$$132 4\pi u(x) = \int_B T(s, x)u(s)dB(s) - \int_B U(s, x)\frac{\partial u(s)}{\partial n_s}dB(s), \quad x \in D \cup B, \quad (12)$$

$$134 4\pi \frac{\partial u(x)}{\partial n_x} = \int_B M(s, x)u(s)dB(s) - \int_B L(s, x)\frac{\partial u(s)}{\partial n_s}dB(s), \quad x \in D \cup B, \quad (13)$$

138 and

$$139 0 = \int_B T(s, x)u(s)dB(s) - \int_B U(s, x)\frac{\partial u(s)}{\partial n_s}dB(s), \quad x \in D^c \cup B, \quad (14)$$

$$141 0 = \int_B M(s, x)u(s)dB(s) - \int_B L(s, x)\frac{\partial u(s)}{\partial n_s}dB(s), \quad x \in D^c \cup B, \quad (15)$$

142 once the kernel is expressed in terms of an appropriate degenerate  
143 form. It is found that the collocation point is categorized to three  
144 positions, domain (Eqs. (2) and (3)), boundary (Eqs. (8) and (9))  
145 and complementary domain (Eqs. (10) and (11)) in the conventional  
146 formulation. After using the degenerate kernel for the null-field  
147 BIEM, both Eqs. (12)–(15) can contain the boundary point. The  
148 resulted linear algebraic systems derived from Eqs. (12)–(15) are  
149 the same [19], i.e. we can move to the boundary either from the  
150 domain point or null-field point. The main reason can be found from  
151 the Appendix A to see how jump terms appear.

### 152 2.4. Expansions of the fundamental solution and boundary density

153 The fundamental solution as previously mentioned is

$$155 U(s, x) = -\frac{e^{-ikr}}{r}, \quad (16)$$

156 where  $r \equiv |s - x|$  is the distance between the source point and the  
157 field point and  $i$  is the imaginary number with  $i^2 = -1$ . To fully uti-  
158 lize the property of spherical geometry, the mathematical tools,  
159 degenerate (separable or finite rank) kernel and spherical harmon-  
160 ics, are utilized for the analytically calculating the boundary  
161 integrals.

#### 162 2.4.1. Degenerate kernel for fundamental solutions

163 In the spherical coordinates, the field point ( $x$ ) and source point  
164 ( $s$ ) can be expressed as  $x = (\rho, \phi, \theta)$  and  $s = (\bar{\rho}, \bar{\phi}, \bar{\theta})$ , respectively.  
165 By employing the addition theorem for separating the source point  
166 and field point, the kernel functions,  $U(s, x)$ ,  $T(s, x)$ ,  $L(s, x)$  and  
167  $M(s, x)$ , are expanded in terms of degenerate kernel as shown  
168 below:

169

$$U(s, x) = \begin{cases} U^i(s, x) = ik \sum_{n=0}^{\infty} (2n+1) \sum_{m=0}^n \varepsilon_m \frac{(n-m)!}{(n+m)!} \cos(m(\phi - \bar{\phi})) \\ \times P_n^m(\cos \theta) P_n^m(\cos \bar{\theta}) j_n(k\rho) h_n^{(2)}(k\bar{\rho}), \quad \bar{\rho} \geq \rho, \\ U^e(s, x) = ik \sum_{n=0}^{\infty} (2n+1) \sum_{m=0}^n \varepsilon_m \frac{(n-m)!}{(n+m)!} \cos(m(\phi - \bar{\phi})) \\ \times P_n^m(\cos \theta) P_n^m(\cos \bar{\theta}) j_n(k\bar{\rho}) h_n^{(2)}(k\rho), \quad \rho > \bar{\rho}, \end{cases} \quad (17)$$

171

$$T(s, x) = \begin{cases} T^i(s, x) = ik^2 \sum_{n=0}^{\infty} (2n+1) \sum_{m=0}^n \varepsilon_m \frac{(n-m)!}{(n+m)!} \cos(m(\phi - \bar{\phi})) \\ \times P_n^m(\cos \theta) P_n^m(\cos \bar{\theta}) j_n(k\rho) h_n^{(2)}(k\bar{\rho}), \quad \bar{\rho} > \rho, \\ T^e(s, x) = ik^2 \sum_{n=0}^{\infty} (2n+1) \sum_{m=0}^n \varepsilon_m \frac{(n-m)!}{(n+m)!} \cos(m(\phi - \bar{\phi})) \\ \times P_n^m(\cos \theta) P_n^m(\cos \bar{\theta}) j'_n(k\bar{\rho}) h_n^{(2)}(k\rho), \quad \rho > \bar{\rho}, \end{cases} \quad (18)$$

174

$$L(s, x) = \begin{cases} L^i(s, x) = ik^2 \sum_{n=0}^{\infty} (2n+1) \sum_{m=0}^n \varepsilon_m \frac{(n-m)!}{(n+m)!} \cos(m(\phi - \bar{\phi})) \\ \times P_n^m(\cos \theta) P_n^m(\cos \bar{\theta}) j'_n(k\rho) h_n^{(2)}(k\bar{\rho}), \quad \bar{\rho} > \rho, \\ L^e(s, x) = ik^2 \sum_{n=0}^{\infty} (2n+1) \sum_{m=0}^n \varepsilon_m \frac{(n-m)!}{(n+m)!} \cos(m(\phi - \bar{\phi})) \\ \times P_n^m(\cos \theta) P_n^m(\cos \bar{\theta}) j_n(k\bar{\rho}) h_n^{(2)}(k\rho), \quad \rho > \bar{\rho}, \end{cases} \quad (19)$$

177

$$M(s, x) = \begin{cases} M^i(s, x) = ik^3 \sum_{n=0}^{\infty} (2n+1) \sum_{m=0}^n \varepsilon_m \frac{(n-m)!}{(n+m)!} \cos(m(\phi - \bar{\phi})) \\ \times P_n^m(\cos \theta) P_n^m(\cos \bar{\theta}) j'_n(k\rho) h_n^{(2)}(k\bar{\rho}), \quad \bar{\rho} \geq \rho, \\ M^e(s, x) = ik^3 \sum_{n=0}^{\infty} (2n+1) \sum_{m=0}^n \varepsilon_m \frac{(n-m)!}{(n+m)!} \cos(m(\phi - \bar{\phi})) \\ \times P_n^m(\cos \theta) P_n^m(\cos \bar{\theta}) j'_n(k\bar{\rho}) h_n^{(2)}(k\rho), \quad \rho > \bar{\rho}, \end{cases} \quad (20)$$

180

where the superscripts “*i*” and “*e*” denote the interior and exterior regions,  $j_n$  and  $h_n^{(2)}$  are the *n*th order spherical Bessel function of the first kind and the *n*th order spherical Hankel function of the second kind, respectively,  $P_n^m$  is the associated Legendre polynomial and  $\varepsilon_m$  is the Neumann factor,

$$\varepsilon_m = \begin{cases} 1, & m = 0, \\ 2, & m = 1, 2, \dots, \infty. \end{cases} \quad (21)$$

It is noted that  $U$  and  $M$  kernels in Eqs. (17) and (20) contain the equal sign of  $\rho = \bar{\rho}$  while  $T$  and  $L$  kernels do not include the equal sign due to discontinuity in Eqs. (18) and (19). Besides, the potential across the boundary is also addressed here. For 2D Laplace and Helmholtz equations, the continuous and jump behavior across the boundary were studied, respectively, in [20,21]. After using the Wronskian property of  $j_m$  and  $y_m$ , we have

$$W(j_m(k\bar{\rho}), y_m(k\bar{\rho})) = i(j_m(k\bar{\rho})y'_m(k\bar{\rho}) - j'_m(k\bar{\rho})y_m(k\bar{\rho})) = \frac{i}{k\bar{\rho}^2}, \quad (22)$$

where  $h_m^{(2)}(k\bar{\rho}) = j(k\bar{\rho}) - iy(k\bar{\rho})$ . The jump behavior is well captured by

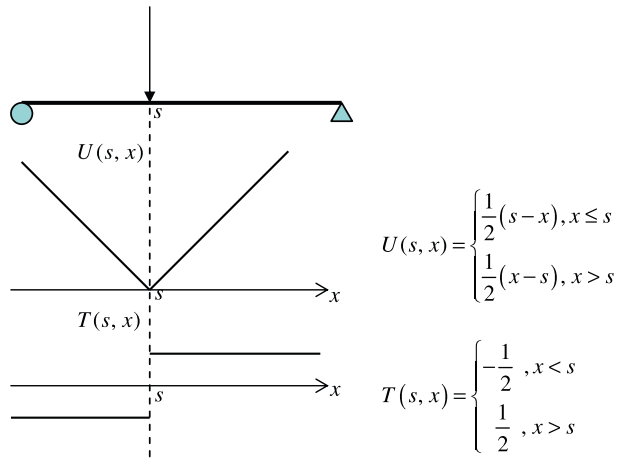


Fig. 2. Jump behavior for a rod case.

$$\int_0^{2\pi} \int_0^\pi [T^i(s, x) - T^e(s, x)] P_n^m(\cos \bar{\theta}) \cos(m\bar{\theta}) \bar{\rho}^2 \sin(m\bar{\theta}) d\bar{\theta} d\bar{\phi} \\ = -4\pi k P_n^m(\cos \theta) \cos(m\phi) \quad (23)$$

Similarly, the potentials due to  $L^i$  and  $L^e$  kernels are discontinuous across the boundary. For clarity, a detailed description is given in Appendix A. For simplicity, we also give a simple example by a rod case to show how the jump appears. The degenerate kernels are shown in Fig. 2.

#### 2.4.2. Spherical harmonics for boundary densities

We used the spherical harmonics to approximate the boundary density and its normal derivative as expressed by

$$u(s) = \sum_{v=0}^{\infty} \sum_{w=0}^v A_{vw} P_v^w(\cos \bar{\theta}) \cos(w\bar{\phi}), \quad s \in B, \quad (24)$$

$$t(s) = \frac{\partial u(s)}{\partial n_s} = \sum_{v=0}^{\infty} \sum_{w=0}^v B_{vw} P_v^w(\cos \bar{\theta}) \cos(w\bar{\phi}), \quad s \in B, \quad (25)$$

where  $A_{vw}$  and  $B_{vw}$  are the unknown coefficients.

### 3. Proof of the existence of spurious eigensolutions for a concentric sphere

In order to fully utilize the geometry of sphere boundary, the potential  $u$  and its normal derivative  $t$  can be approximated by employing the spherical harmonic functions. Therefore, the following expressions can be obtained

$$u_1(s) = \sum_{v=0}^{\infty} \sum_{w=0}^v A_{vw}^1 P_v^w(\cos \bar{\theta}) \cos(w\bar{\phi}), \quad s \in B_1, \quad (26)$$

$$u_2(s) = \sum_{v=0}^{\infty} \sum_{w=0}^v A_{vw}^2 P_v^w(\cos \bar{\theta}) \cos(w\bar{\phi}), \quad s \in B_2, \quad (27)$$

$$t_1(s) = \sum_{v=0}^{\infty} \sum_{w=0}^v B_{vw}^1 P_v^w(\cos \bar{\theta}) \cos(w\bar{\phi}), \quad s \in B_1, \quad (28)$$

$$t_2(s) = \sum_{v=0}^{\infty} \sum_{w=0}^v B_{vw}^2 P_v^w(\cos \bar{\theta}) \cos(w\bar{\phi}), \quad s \in B_2, \quad (29)$$

where  $A_{vw}^i$  and  $B_{vw}^i$  are the spherical coefficients on  $B_i$  ( $i = 1, 2$ ). By substituting Eqs. (26)–(29) into the null-field integral equations and moving the null-field point to the boundary, we have

$$\begin{aligned}
0 = & \int_0^{2\pi} \int_0^\pi \sum_{n=0}^\infty \sum_{m=0}^n \sum_{v=0}^\infty \sum_{w=0}^v ik^2 \epsilon_m A_{vw}^1 (2n+1) \\
& \times \frac{(n-m)!}{(n+m)!} j_n(k\rho) h_n^{(2)}(kR_1) P_n^m(\cos(\theta)) \cos(m(\phi - \bar{\phi})) \\
& \times \cos(w\bar{\phi}) (P_n^m(\cos(\bar{\theta})) P_v^w(\cos(\bar{\theta})) \sin(\bar{\theta})) R_1^2 d\bar{\theta} d\bar{\phi} \\
& - \int_0^{2\pi} \int_0^\pi \sum_{n=0}^\infty \sum_{m=0}^n \sum_{v=0}^\infty \sum_{w=0}^v ik \epsilon_m B_{vw}^1 (2n+1) \\
& \times \frac{(n-m)!}{(n+m)!} j_n(k\rho) h_n^{(2)}(kR_1) P_n^m(\cos(\theta)) \cos(m(\phi - \bar{\phi})) \\
& \times \cos(w\bar{\phi}) (P_n^m(\cos(\bar{\theta})) P_v^w(\cos(\bar{\theta})) \sin(\bar{\theta})) R_1^2 d\bar{\theta} d\bar{\phi} \\
& + \int_0^{2\pi} \int_0^\pi \sum_{n=0}^\infty \sum_{m=0}^n \sum_{v=0}^\infty \sum_{w=0}^v ik^2 \epsilon_m A_{vw}^2 (2n+1) \\
& \times \frac{(n-m)!}{(n+m)!} j_n(k\rho) h_n^{(2)}(kR_2) P_n^m(\cos(\theta)) \cos(m(\phi - \bar{\phi})) \\
& \times \cos(w\bar{\phi}) (P_n^m(\cos(\bar{\theta})) P_v^w(\cos(\bar{\theta})) \sin(\bar{\theta})) R_2^2 d\bar{\theta} d\bar{\phi} \\
& - \int_0^{2\pi} \int_0^\pi \sum_{n=0}^\infty \sum_{m=0}^n \sum_{v=0}^\infty \sum_{w=0}^v ik \epsilon_m B_{vw}^2 (2n+1) \\
& \times \frac{(n-m)!}{(n+m)!} j_n(k\rho) h_n^{(2)}(kR_2) P_n^m(\cos(\theta)) \cos(m(\phi - \bar{\phi})) \\
& \times \cos(w\bar{\phi}) (P_n^m(\cos(\bar{\theta})) P_v^w(\cos(\bar{\theta})) \sin(\bar{\theta})) R_2^2 d\bar{\theta} d\bar{\phi}. \quad (30)
\end{aligned}$$

When the field point is located on the outer boundary  $B_2$ , we have

$$\begin{aligned}
0 = & \int_0^{2\pi} \int_0^\pi \sum_{n=0}^\infty \sum_{m=0}^n \sum_{v=0}^\infty \sum_{w=0}^v ik^2 \epsilon_m A_{vw}^1 (2n+1) \\
& \times \frac{(n-m)!}{(n+m)!} j'_n(kR_1) h_n^{(2)}(k\rho) P_n^m(\cos(\theta)) \cos(m(\phi - \bar{\phi})) \\
& \times \cos(w\bar{\phi}) (P_n^m(\cos(\bar{\theta})) P_v^w(\cos(\bar{\theta})) \sin(\bar{\theta})) R_1^2 d\bar{\theta} d\bar{\phi} \\
& - \int_0^{2\pi} \int_0^\pi \sum_{n=0}^\infty \sum_{m=0}^n \sum_{v=0}^\infty \sum_{w=0}^v ik \epsilon_m B_{vw}^1 (2n+1) \\
& \times \frac{(n-m)!}{(n+m)!} j_n(kR_1) h_n^{(2)}(k\rho) P_n^m(\cos(\theta)) \cos(m(\phi - \bar{\phi})) \\
& \times \cos(w\bar{\phi}) (P_n^m(\cos(\bar{\theta})) P_v^w(\cos(\bar{\theta})) \sin(\bar{\theta})) R_1^2 d\bar{\theta} d\bar{\phi} \\
& + \int_0^{2\pi} \int_0^\pi \sum_{n=0}^\infty \sum_{m=0}^n \sum_{v=0}^\infty \sum_{w=0}^v ik^2 \epsilon_m A_{vw}^2 (2n+1) \\
& \times \frac{(n-m)!}{(n+m)!} j'_n(kR_2) h_n^{(2)}(k\rho) P_n^m(\cos(\theta)) \cos(m(\phi - \bar{\phi})) \\
& \times \cos(w\bar{\phi}) (P_n^m(\cos(\bar{\theta})) P_v^w(\cos(\bar{\theta})) \sin(\bar{\theta})) R_2^2 d\bar{\theta} d\bar{\phi} \\
& - \int_0^{2\pi} \int_0^\pi \sum_{n=0}^\infty \sum_{m=0}^n \sum_{v=0}^\infty \sum_{w=0}^v ik \epsilon_m B_{vw}^2 (2n+1) \\
& \times \frac{(n-m)!}{(n+m)!} j_n(kR_2) h_n^{(2)}(k\rho) P_n^m(\cos(\theta)) \cos(m(\phi - \bar{\phi})) \\
& \times \cos(w\bar{\phi}) (P_n^m(\cos(\bar{\theta})) P_v^w(\cos(\bar{\theta})) \sin(\bar{\theta})) R_2^2 d\bar{\theta} d\bar{\phi}. \quad (31)
\end{aligned}$$

For the Dirichlet problem, Eqs. (30) and (31) can be reduced to

$$\begin{aligned}
0 = & \sum_{n=0}^\infty \sum_{m=0}^n a^2 k B_{nm}^1 j_n(ka) h_n^{(2)}(ka) P_n^m(\cos(\theta)) \cos(m\phi) \\
& + \sum_{n=0}^\infty \sum_{m=0}^n b^2 k B_{nm}^2 j_n(ka) h_n^{(2)}(kb) P_n^m(\cos(\theta)) \cos(m\phi), \quad (32)
\end{aligned}$$

$$\begin{aligned}
0 = & \sum_{n=0}^\infty \sum_{m=0}^n a^2 k B_{nm}^1 j_n(ka) h_n^{(2)}(kb) P_n^m(\cos(\theta)) \cos(m\phi) \\
& + \sum_{n=0}^\infty \sum_{m=0}^n b^2 k B_{nm}^2 j_n(kb) h_n^{(2)}(kb) P_n^m(\cos(\theta)) \cos(m\phi). \quad (33)
\end{aligned}$$

According to Eqs. (32) and (33), the spherical coefficients,  $B_{nm}^1$  and  $B_{nm}^2$ , satisfy the relation as follows:

$$B_{nm}^2 = -\frac{a^2 j_n(ka) h_n^{(2)}(ka)}{b^2 j_n(ka) h_n^{(2)}(kb)} B_{nm}^1, \quad (34)$$

$$B_{nm}^2 = -\frac{a^2 j_n(ka) h_n^{(2)}(kb)}{b^2 j_n(kb) h_n^{(2)}(kb)} B_{nm}^1. \quad (35)$$

To seek the nontrivial data for the spherical coefficients  $B_{nm}^1$  and  $B_{nm}^2$ , we obtain the eigenequation:

$$j_n(ka) h_n^{(2)}(kb) [j_n(kb) h_n^{(2)}(ka) - j_n(ka) h_n^{(2)}(kb)] = 0 \quad (36)$$

For the Neumann problem, the Eqs. (30) and (31) are reduced to

$$0 = \sum_{n=0}^\infty \sum_{m=0}^n a^2 A_{nm}^1 j_n(ka) h_n^{(2)}(ka) + \sum_{n=0}^\infty \sum_{m=0}^n b^2 A_{nm}^2 j_n(ka) h_n^{(2)}(kb), \quad (37)$$

$$0 = \sum_{n=0}^\infty \sum_{m=0}^n a^2 A_{nm}^1 j_n(ka) h_n^{(2)}(kb) + \sum_{n=0}^\infty \sum_{m=0}^n b^2 A_{nm}^2 j_n(kb) h_n^{(2)}(kb). \quad (38)$$

According to Eqs. (37) and (38), the spherical coefficients  $A_{nm}^1$  and  $A_{nm}^2$  satisfy the relations:

$$A_{nm}^2 = -\frac{a^2 j_n(ka) h_n^{(2)}(ka)}{b^2 j_n(ka) h_n^{(2)}(kb)} A_{nm}^1, \quad (39)$$

$$A_{nm}^2 = -\frac{a^2 j'_n(ka) h_n^{(2)}(kb)}{b^2 j'_n(kb) h_n^{(2)}(kb)} A_{nm}^1. \quad (40)$$

To seek the nontrivial data for the spherical coefficients  $A_{nm}^1$  and  $A_{nm}^2$ , we obtain the eigenequation:

$$j_n(ka) h_n^{(2)}(kb) [j'_n(kb) h_n^{(2)}(ka) - j'_n(ka) h_n^{(2)}(kb)] = 0. \quad (41)$$

According to Eqs. (36) and (41), the spurious eigenequation of the singular formulation is  $j_n(ka) = 0$ , which is also the true eigenequation of the sphere of radius  $a$  with the fixed boundary condition. The latter parts in the bracket of Eqs. (36) and (41) are the true eigenequations,

$$j_n(kb) h_n^{(2)}(ka) - j_n(ka) h_n^{(2)}(kb) = 0 \quad \text{for the Dirichlet problem} \quad (42)$$

$$j'_n(kb) h_n^{(2)}(ka) - j'_n(ka) h_n^{(2)}(kb) = 0 \quad \text{for the Neumann problem} \quad (43)$$

The spurious and true eigenequations of the concentric sphere subject to various boundary conditions are listed in Table 1. It is interesting to find that spurious eigenvalue of  $UT$  (singular) formulation results in trivial outer boundary modes for the **fixed-fixed** case. Besides, spurious eigenvalue of  $LM$  (hypersingular) formulation results in the trivial outer boundary modes of **free-free** case.

#### 4. Proof of the existence for the spurious eigensolutions of the eccentric sphere

In order to prove that the spurious eigensolutions of a concentric sphere satisfy the BIE by collocating the inner and outer boundary points, we first derive the true eigensolutions of a sphere subject to the Dirichlet boundary condition. Now, we consider the sphere with a radius  $a$  in the continuous system. By using the null-field integral equation and collocating the point on the boundary, we obtain the true eigenequation

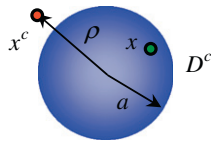
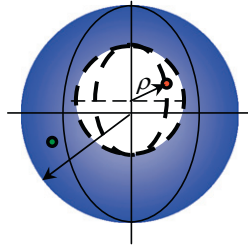
$$j_n(ka) = 0, \quad (44)$$

and the corresponding true eigenmode is  $B_{nm}$ , where  $\sum |B_{nm}| \neq 0$ . By collocating the point in the complementary domain ( $x^c \in D^c$ ) as shown in Fig. 3, the null-field equation yields

**Table 1**

Eigensolutions and boundary modes for the concentric sphere subject to different boundary conditions.

	Solution	BC			
		Fixed-fixed $u_1 = u_2 = 0$	Free-fixed $t_1 = u_2 = 0$	Fixed-free $u_1 = t_2 = 0$	Free-free $t_1 = t_2 = 0$
UT formulation	True eigenequation	$j_n(ka)y_n(kb) - j_n(kb)y_n(ka) = 0$	$j_n(ka)y_n(kb) - j_n(kb)y'_n(ka) = 0$	$j_n(ka)y'_n(kb) - j'_n(kb)y_n(ka) = 0$	$j'_n(ka)y'_n(kb) - j'_n(kb)y'_n(ka) = 0$
	Spurious eigenequation	$j_n(ka) = 0$	$j_n(ka) = 0$	$j_n(ka) = 0$	$j_n(ka) = 0$
	Inner boundary mode	$\sum \sum  B_{nm}  \neq 0$	$\sum \sum  A_{nm}  \neq 0$	$\sum \sum  B_{nm}  \neq 0$	$\sum \sum  A_{nm}  \neq 0$
	Outer boundary mode	$B_{nm}^2 = \frac{a^2 j_n(ka)}{b^2 j_n(kb)} B_{nm}^1$	$B_{nm}^2 = \frac{a^2 j'_n(ka)}{b^2 j'_n(kb)} A_{nm}^1$	$A_{nm}^2 = \frac{a^2 j_n(ka)}{b^2 j_n(kb)} B_{nm}^1$	$A_{nm}^2 = \frac{a^2 j'_n(ka)}{b^2 j'_n(kb)} A_{nm}^1$
LM formulation	True eigenequation	$j_n(ka)y_n(kb) - j_n(kb)y_n(ka) = 0$	$j'_n(ka)y_n(kb) - j_n(kb)y'_n(ka) = 0$	$j_n(ka)y'_n(kb) - j'_n(kb)y_n(ka) = 0$	$j'_n(ka)y'_n(kb) - j'_n(kb)y'_n(ka) = 0$
	Spurious eigenequation	$j'_n(ka) = 0$	$j'_n(ka) = 0$	$j'_n(ka) = 0$	$j'_n(ka) = 0$
	Inner boundary mode	$\sum \sum  B_{nm}  \neq 0$	$\sum \sum  A_{nm}  \neq 0$	$\sum \sum  B_{nm}  \neq 0$	$\sum \sum  A_{nm}  \neq 0$
	Outer boundary mode	$B_{nm}^2 = \frac{a^2 j_n(ka)}{b^2 j_n(kb)} B_{nm}^1$	$B_{nm}^2 = \frac{a^2 j'_n(ka)}{b^2 j'_n(kb)} A_{nm}^1$	$A_{nm}^2 = \frac{a^2 j_n(ka)}{b^2 j_n(kb)} B_{nm}^1$	$A_{nm}^2 = \frac{a^2 j'_n(ka)}{b^2 j'_n(kb)} A_{nm}^1$

**Fig. 3.** Collocation point on the sphere boundary from the null-field point ( $\rho = a^+$ ).**Fig. 4.** Collocation point of the eccentric sphere ( $\rho = a^-$ ).

$$0 = \int_{B_1} U^e(s, x^c) t(s) dB(s), \quad x^c \in D^c. \quad (45)$$

We can obtain the null-field response for  $x^c$  as shown below

$$B_{nm}^1 j_n(ka) h_n^{(2)}(ka^+) P_n^m(\cos(\theta)) \cos(m\phi) = 0, \quad (46)$$

where  $n$  and  $m$  belong to nature number and  $k$  satisfies Eq. (44).Secondly, we consider the spherical case with the fixed-fixed boundary condition as shown in Fig. 4. By selecting a nontrivial inner boundary mode for the boundary mode and trivial outer boundary mode, we have  $j_n(ka) = 0$  and

$$\begin{cases} B_{nm}^1 \\ B_{nm}^2 \end{cases} = \begin{cases} B_{nm} \\ 0 \end{cases} \quad (47)$$

This indicates that spurious eigenvalues of  $j_n(ka) = 0$  and the non-trivial boundary mode of Eq. (47) satisfy Eqs. (32) and (33) due to  $U^i(s, a^-) = U^e(x, a^+)$ . Therefore, spurious eigenvalues in conjunction with the trivial outer boundary mode happen to be the true eigenvalue of the domain bounded by the inner boundary. Similarly,

concentric sphere subjected to the Neumann boundary condition by using the hypersingular formulation results in the trivial outer boundary mode.

## 5. SVD technique for extracting out true and spurious eigenvalues by using updating terms and updating documents

### 5.1. Method of extracting the true eigensolutions (updating terms)

SVD technique is an important tool in the linear algebra. The matrix  $[A]$  with a dimension  $M$  by  $N$  can be decomposed into a product of the unitary matrix  $[\Phi]$  ( $M$  by  $M$ ), the diagonal matrix  $[\Sigma]$  ( $M$  by  $N$ ) with positive or zero elements, and the unitary matrix  $[\Psi]$  ( $N$  by  $N$ ) as follows:

$$[A]_{M \times N} = [\Phi]_{M \times M} [\Sigma]_{M \times N} [\Psi]_{N \times N}^H, \quad (48)$$

where the superscript “ $H$ ” is the Hermitian operator,  $[\Phi]$  and  $[\Psi]$  are both unitary matrices that their column vectors which satisfy

$$\sum_i \phi_i^H \cdot \phi_j = \delta_{ij}, \quad (49)$$

$$\sum_i \psi_i^H \cdot \psi_j = \delta_{ij}, \quad (50)$$

in which  $[\Phi]^H [\Phi] = [I]_{M \times M}$  and  $[\Psi]^H [\Psi] = [I]_{N \times N}$ . For the eigenproblem, we can obtain a nontrivial solution for the homogeneous system from a column vector  $\{\psi_i\}$  of  $[\Psi]$  when the singular value ( $\sigma_i$ ) is zero. For the BIEM, we have

*Singular formulation (UT method)*

$$[U^e]\{u\} = [U^e]\{t\} = \{0\}, \quad (51)$$

*Hypersingular formulation (LM method)*

$$[M^e]\{u\} = [L^e]\{t\} = \{0\}, \quad (52)$$

where  $\{u\}$  and  $\{t\}$  are the boundary excitations. For the Dirichlet problem, Eqs. (51) and (52) can be combined to have

$$\begin{bmatrix} U^e \\ L^e \end{bmatrix}\{t\} = \{0\}. \quad (53)$$

By using the SVD technique, the two submatrices in Eqs. (51) and (52) can be decomposed into

$$[\mathbf{U}^e] = [\Phi^{(U)}][\Sigma^{(U)}][\Psi^{(U)}]^H \quad \text{or} \quad [\mathbf{U}^e] = \sum_j \sigma_j^{(U)} \{\phi_j^{(U)}\} \{\psi_j^{(U)}\}^H, \quad (54)$$

$$[\mathbf{L}^e] = [\Phi^{(L)}][\Sigma^{(L)}][\Psi^{(L)}]^H \quad \text{or} \quad [\mathbf{L}^e] = \sum_j \sigma_j^{(L)} \{\phi_j^{(L)}\} \{\psi_j^{(L)}\}^H, \quad (55)$$

where the superscripts,  $(U)$  and  $(L)$ , denote the corresponding matrices. For the linear algebraic system,  $\{t\}$  is a column vector of  $\{\psi_i\}$  in the matrix  $[\Psi]$  corresponding to the zero singular value ( $\sigma_i = 0$ ). By setting  $\{t\}$  as a vector of  $\{\psi_i\}$  in the right unitary matrix for the true eigenvalue  $k_t$ , Eqs. (51) and (52) reduces to

$$[\mathbf{U}^e(k_t)]\{\psi_i\} = \{0\}, \quad (56)$$

$$[\mathbf{L}^e(k_t)]\{\psi_i\} = \{0\}. \quad (57)$$

According to Eqs. (54)–(57), we have

$$\sigma_j^{(U)} \{\phi_j^{(U)}\} = \{0\}, \quad (58)$$

$$\sigma_j^{(L)} \{\phi_j^{(L)}\} = \{0\}. \quad (59)$$

We can easily extract out the true eigenvalues,  $\sigma_j^{(U)} = \sigma_j^{(L)} = \{0\}$ , since there exists the same eigensolution ( $\{t\} = \{\psi_i\}$ ) for the

**Table 2a**

SVD structure of the four influence matrices for the Dirichlet and Neumann problems in the case of true eigenvalue.

	Dirichlet problem ( $k = k_T^D$ )		Neumann problem ( $k = k_T^N$ )	
	$[\Phi^U]\begin{bmatrix} 0 & \cdot & \cdot \\ \cdot & \ddots & \cdot \\ \cdot & \cdot & \ddots \end{bmatrix}[\phi_i^D \dots]^H$	$[\Phi^T][\Sigma^T][\Psi^T]^H$	$[\Phi^U]\begin{bmatrix} 0 & \cdot & \cdot \\ \cdot & \ddots & \cdot \\ \cdot & \cdot & \ddots \end{bmatrix}[\phi_i^N \dots]^H$	$[\Phi^T]\begin{bmatrix} 0 & \cdot & \cdot \\ \cdot & \ddots & \cdot \\ \cdot & \cdot & \ddots \end{bmatrix}[\phi_i^N \dots]^H$
True eigenvalue $k_T$ ( $k_T^D, k_T^N$ )	$\boxed{U} \boxed{T}$	$\boxed{L} \boxed{M}$	$\boxed{U} \boxed{T}$	$\boxed{L} \boxed{M}$

where  $k_T^D$  and  $k_T^N$  devotes the true eigenvalues for the Dirichlet and Neumann problems, respectively.

**Table 2b**

SVD structure of the four influence matrices by using the UT singular formulation and LM hypersingular formulation in the case of spurious eigenvalue.

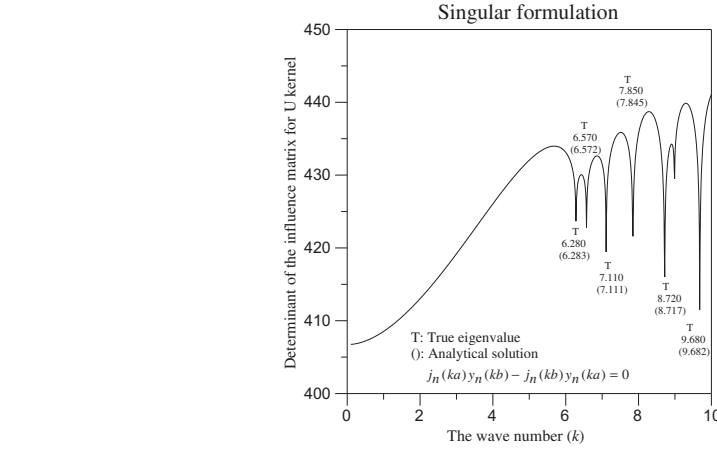
	UT singular formulation ( $k = k_s^{UT}$ )		LM hypersingular formulation ( $k = k_s^{LM}$ )	
	Dirichlet	Neumann	Dirichlet	Neumann
Spurious eigenvalue $k_s$ ( $k_s^{UT}, k_s^{LM}$ )	$[\phi_i^{UT} \dots] \begin{bmatrix} 0 & \cdot & \cdot \\ \cdot & \ddots & \cdot \\ \cdot & \cdot & \ddots \end{bmatrix} \begin{bmatrix} \phi_i^D & \dots \\ \{0\} & \dots \end{bmatrix}^H$	$[\phi_i^{UT} \dots] \begin{bmatrix} 0 & \cdot & \cdot \\ \cdot & \ddots & \cdot \\ \cdot & \cdot & \ddots \end{bmatrix} [\Psi^T]^H$	$[\phi_i^{LM} \dots] \begin{bmatrix} 0 & \cdot & \cdot \\ \cdot & \ddots & \cdot \\ \cdot & \cdot & \ddots \end{bmatrix} [\Psi^L]^H$	$[\phi_i^{LM} \dots] \begin{bmatrix} 0 & \cdot & \cdot \\ \cdot & \ddots & \cdot \\ \cdot & \cdot & \ddots \end{bmatrix} \begin{bmatrix} \phi_i^N & \dots \\ \{0\} & \dots \end{bmatrix}^H$

where  $k_s^{UT}$  and  $k_s^{LM}$  devotes the spurious eigenvalues by using UT singular and LM hypersingular formulation, respectively.

$$[\mathbf{L}^e(k_s)]^H \{\phi_i\} = \{0\} \quad \text{for the Dirichlet problem,} \quad (63)$$

$$[\mathbf{M}^e(k_s)]^H \{\phi_i\} = \{0\} \quad \text{for the Neumann problem,} \quad (64)$$

according to the Fredholm alternative theorem. By substituting Eq. (61) into Eqs. (62)–(64), we have

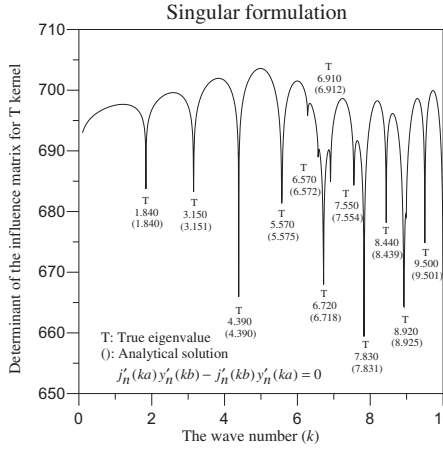


(a) Determinant versus the wave number by using the singular formulation for the Dirichlet condition.

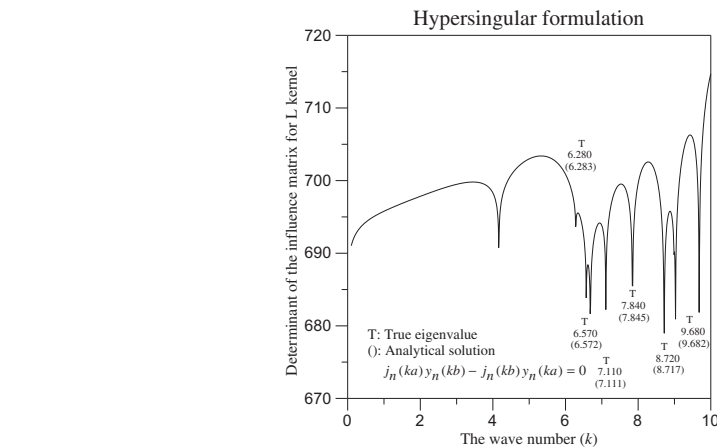
$$\{u\}^H [\mathbf{M}^e(k_s)]^H \{\phi_i\} = \{0\} \quad \text{for the Dirichlet problem,} \quad (65)$$

$$\{t\}^H [\mathbf{L}^e(k_s)]^H \{\phi_i\} = \{0\} \quad \text{for the Neumann problem.} \quad (66)$$

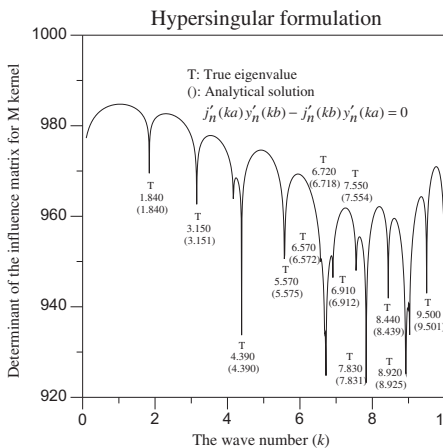
Since  $\{u\}$  and  $\{t\}$  can be arbitrary boundary excitation for the Dirichlet problem and Neumann problem, respectively, this yields



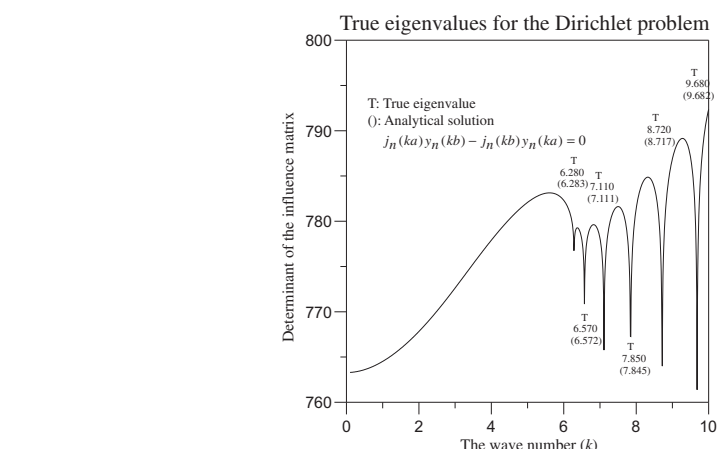
(d) Determinant versus the wave numbers by using the singular formulation for the Neumann condition.



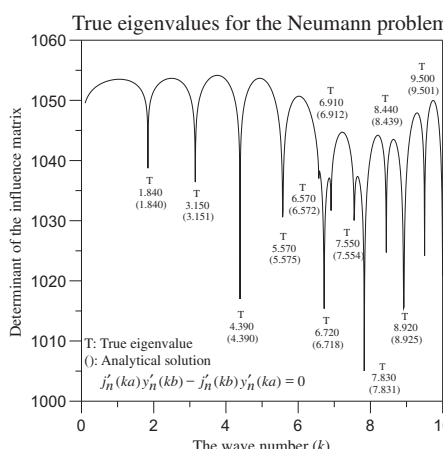
(b) Determinant versus the wave number by using the hypersingular formulation for the Dirichlet condition.



(e) Determinant versus the wave number by using the hypersingular formulation for the Neumann condition.



(c) Extraction of true eigenvalues for the Dirichlet problem by using the SVD updating terms.



(f) Extraction of true eigenvalues for the Neumann problem by using the SVD updating terms.

Fig. 5. True eigenvalues for a concentric sphere by using the SVD updating terms ( $a = 0.5$  and  $b = 1.0$ ).

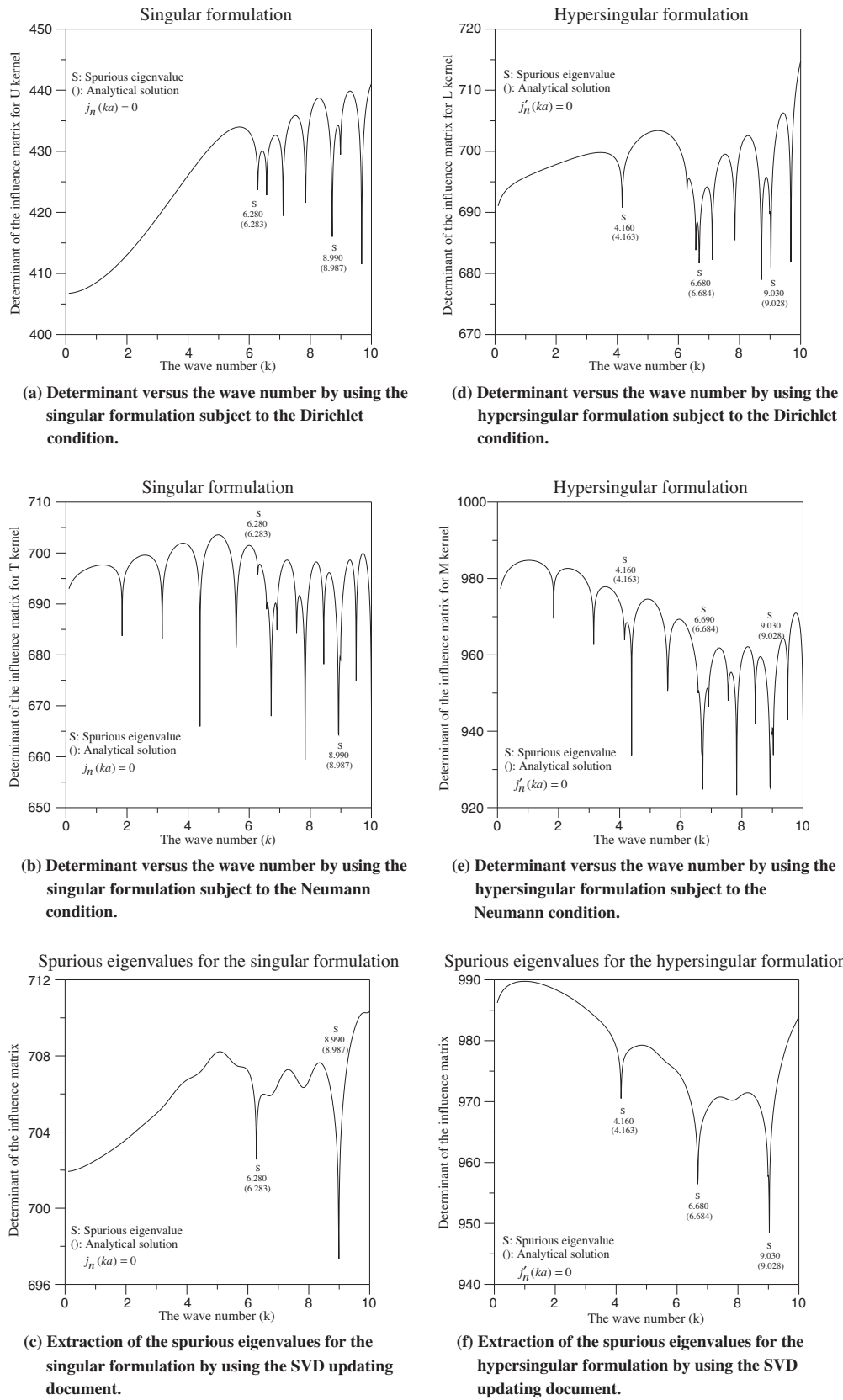


**Fig. 6.** Extraction of spurious eigenvalues for a concentric sphere by using the SVD updating documents ( $a = 0.5$  and  $b = 1.0$ ).

$$[\mathbf{M}^e(k_s)]^H \{\phi_i\} = \{0\} \quad \text{for the Dirichlet problem,} \quad (67)$$

$$[\mathbf{L}^e(k_s)]^H \{\phi_i\} = \{0\} \quad \text{for the Neumann problem.} \quad (68)$$

By combining Eq. (63) with Eq. (67) for the Dirichlet problem, we have

$$\begin{bmatrix} [\mathbf{L}^e]^H \\ [\mathbf{M}^e]^H \end{bmatrix} \{\phi_i\} = \{0\} \quad \text{or} \quad \{\phi_i\}^H [\mathbf{L}^e] [\mathbf{M}^e] = \{0\}. \quad (69)$$

It indicates that two matrices have the same spurious boundary mode  $\{\phi_i\}$  corresponding to the  $i$ th zero singular values. By using the SVD technique, two matrices in Eq. (69) can be decomposed into

$$[\mathbf{L}^e]^H = [\Psi^{(L)}][\Sigma^{(L)}][\Phi^{(L)}]^H \quad \text{or} \quad [\mathbf{L}^e] = \sum_j \sigma_j^{(L)} \{\psi_j^{(L)}\} \{\phi_j^{(L)}\}^H, \quad (70)$$

$$[\mathbf{M}^e]^H = [\Psi^{(M)}][\Sigma^{(M)}][\Phi^{(M)}]^H \quad \text{or} \quad [\mathbf{M}^e] = \sum_j \sigma_j^{(M)} \{\psi_j^{(M)}\} \{\phi_j^{(M)}\}^H. \quad (71)$$

By substituting Eqs. (70) and (71) into Eqs. (65) and (66), we have

$$\sigma_j^{(L)} \{\psi_j^{(L)}\} = \{0\}, \quad (72)$$

$$\sigma_j^{(M)} \{\psi_j^{(M)}\} = \{0\}. \quad (73)$$

We can easily extract out the spurious eigenvalues since there exists the same spurious boundary mode  $\{\phi_i\}$  corresponding the  $i$ th zero singular value,  $\sigma_i^{(L)} = \sigma_i^{(M)} = 0$ . Similarly, the spurious eigenvalue parasitized in the UT formulation can be obtained by using SVD updating documents. To summarize the SVD structure for the four influence matrices, Tables 2a and 2b show that the spurious and true boundary modes are imbedded in the left and right unitary vectors, respectively. Besides, the nontrivial interior boundary mode and trivial outer boundary mode are also given in Table 2b.

## 6. Illustrative examples and discussion

*Case 1: A concentric sphere subject to the Dirichlet boundary condition ( $\mathbf{u}_1 = \mathbf{u}_2 = \mathbf{0}$ ) using the present approach.*

A concentric case with radii  $a$  and  $b$  ( $a = 0.5$  m and  $b = 1.0$  m) is shown in Fig. 1. The analytical solution can be obtained by using the null-field integral formulation, degenerate kernel and spherical harmonics. The common drop locations in Fig. 5a and b indicate the true eigenvalues. We employ the SVD updating term  $\begin{bmatrix} U \\ L \end{bmatrix}$  to extract the true eigenvalues for the Dirichlet problem as shown in Fig. 5c. It is found that all the spurious eigenvalues are filtered out. The results agree well with the previous solutions.

## Appendix A

	$U(s, x)$ and $\int_B U(s, x)t(s)dB(s)$	$T(s, x)$ and $\int_B T(s, x)u(s)dB(s)$
Degenerate kernel	$U(s, x) = \begin{cases} U^i(s, x) = ik \sum_{n=0}^{\infty} (2n+1) \sum_{m=0}^n \varepsilon_m \frac{(n-m)!}{(n+m)!} \cos(m(\phi - \bar{\phi})) \\ \quad \times P_n^m(\cos \theta) P_n^m(\cos \bar{\theta}) j_n(k\rho) h_n^{(2)}(k\bar{\rho}), \quad \bar{\rho} \geq \rho, \\ U^e(s, x) = ik \sum_{n=0}^{\infty} (2n+1) \sum_{m=0}^n \varepsilon_m \frac{(n-m)!}{(n+m)!} \cos(m(\phi - \bar{\phi})) \\ \quad \times P_n^m(\cos \theta) P_n^m(\cos \bar{\theta}) j_n(k\bar{\rho}) h_n^{(2)}(k\rho), \quad \rho > \bar{\rho}. \end{cases}$	$T(s, x) = \begin{cases} T^i(s, x) = ik^2 \sum_{n=0}^{\infty} (2n+1) \sum_{m=0}^n \varepsilon_m \frac{(n-m)!}{(n+m)!} \cos(m(\phi - \bar{\phi})) \\ \quad \times P_n^m(\cos \theta) P_n^m(\cos \bar{\theta}) j_n(k\rho) h_n^{(2)}(k\bar{\rho}), \quad \bar{\rho} > \rho, \\ T^e(s, x) = ik^2 \sum_{n=0}^{\infty} (2n+1) \sum_{m=0}^n \varepsilon_m \frac{(n-m)!}{(n+m)!} \cos(m(\phi - \bar{\phi})) \\ \quad \times P_n^m(\cos \theta) P_n^m(\cos \bar{\theta}) j_n'(k\bar{\rho}) h_n^{(2)}(k\rho), \quad \rho > \bar{\rho}. \end{cases}$
Orthogonal process	$U(s, x) = \begin{cases} \int_0^{2\pi} \int_0^\pi ik \sum_{n=0}^{\infty} (2n+1) \sum_{m=0}^n \varepsilon_m \frac{(n-m)!}{(n+m)!} \cos(m(\phi - \bar{\phi})) \\ \quad \times P_n^m(\cos \theta) P_n^m(\cos \bar{\theta}) j_n(k\rho) h_n^{(2)}(k\bar{\rho}) \\ \quad \times P_n^m(\cos \bar{\theta}) \cos(m\bar{\phi}) \bar{\rho}^2 \sin(m\bar{\theta}) d\bar{\theta} d\bar{\phi} \\ = 4\pi k i \bar{\rho}^2 j_n(k\rho) h_n^{(2)}(k\bar{\rho}) P_n^m(\cos \theta) \cos(m\phi), \quad \bar{\rho} \geq \rho, \\ \int_0^{2\pi} \int_0^\pi ik \sum_{n=0}^{\infty} (2n+1) \sum_{m=0}^n \varepsilon_m \frac{(n-m)!}{(n+m)!} \cos(m(\phi - \bar{\phi})) \\ \quad \times P_n^m(\cos \theta) P_n^m(\cos \bar{\theta}) j_n(k\bar{\rho}) h_n^{(2)}(k\rho) \\ \quad \times P_n^m(\cos \bar{\theta}) \cos(m\bar{\phi}) \bar{\rho}^2 \sin(m\bar{\theta}) d\bar{\theta} d\bar{\phi} \\ = 4\pi k i \bar{\rho}^2 j_n(k\bar{\rho}) h_n^{(2)}(k\rho) P_n^m(\cos \theta) \cos(m\phi), \quad \bar{\rho} < \rho. \end{cases}$	$T(s, x) = \begin{cases} T^i(s, x) = \int_0^{2\pi} \int_0^\pi ik^2 \sum_{n=0}^{\infty} (2n+1) \sum_{m=0}^n \varepsilon_m \frac{(n-m)!}{(n+m)!} \cos(m(\phi - \bar{\phi})) \\ \quad \times P_n^m(\cos \theta) P_n^m(\cos \bar{\theta}) j_n(k\rho) h_n^{(2)}(k\bar{\rho}) \\ \quad \times P_n^m(\cos \bar{\theta}) \cos(m\bar{\phi}) \bar{\rho}^2 \sin(m\bar{\theta}) d\bar{\theta} d\bar{\phi} \\ = 4\pi k^2 i \bar{\rho}^2 j_n(k\rho) h_n^{(2)}(k\bar{\rho}) P_n^m(\cos \theta) \cos(m\phi), \quad \bar{\rho} > \rho, \\ T^e(s, x) = \int_0^{2\pi} \int_0^\pi ik^2 \sum_{n=0}^{\infty} (2n+1) \sum_{m=0}^n \varepsilon_m \frac{(n-m)!}{(n+m)!} \cos(m(\phi - \bar{\phi})) \\ \quad \times P_n^m(\cos \theta) P_n^m(\cos \bar{\theta}) j_n'(k\bar{\rho}) h_n^{(2)}(k\rho) \\ \quad \times P_n^m(\cos \bar{\theta}) \cos(m\bar{\phi}) \bar{\rho}^2 \sin(m\bar{\theta}) d\bar{\theta} d\bar{\phi} \\ = 4\pi k^2 i \bar{\rho}^2 j_n'(k\bar{\rho}) h_n^{(2)}(k\rho) P_n^m(\cos \theta) \cos(m\phi), \quad \bar{\rho} < \rho. \end{cases}$

(continued on next page)

**Appendix A (continued)**

	$U(s, x)$ and $\int_B U(s, x)t(s)dB(s)$	$T(s, x)$ and $\int_B T(s, x)u(s)dB(s)$
Limit $\rho \rightarrow \bar{\rho}$	$\begin{cases} 4\pi k i \bar{\rho}^2 j_n(k\bar{\rho}) h_n^{(2)}(k\bar{\rho}) P_n^m(\cos \theta) \cos(m\phi), & \bar{\rho} \geq \rho, \\ 4\pi k i \bar{\rho}^2 j_n(k\bar{\rho}) h_n^{(2)}(k\bar{\rho}) P_n^m(\cos \theta) \cos(m\phi), & \bar{\rho} < \rho. \end{cases} \text{(Continuous for } \bar{\rho}^- < \rho < \bar{\rho}^+\text{)}$	$\begin{cases} 4\pi k^2 i \bar{\rho}^2 j_n(k\bar{\rho}) h_n^{(2)}(k\bar{\rho}) P_n^m(\cos \theta) \cos(m\phi), & \bar{\rho} > \rho, \\ 4\pi k^2 i \bar{\rho}^2 j_n(k\bar{\rho}) h_n^{(2)}(k\bar{\rho}) P_n^m(\cos \theta) \cos(m\phi), & \bar{\rho} < \rho. \end{cases} \text{(Jump for } \bar{\rho}^- < \rho < \bar{\rho}^+ \text{ is } 4\pi k \sum_{n=0}^{\infty} \sum_{m=0}^n P_n^m(\cos \theta) \cos(m\phi))$
Degenerate kernel	$L(s, x) = \begin{cases} L^i(s, x) = ik^2 \sum_{n=0}^{\infty} (2n+1) \sum_{m=0}^n \varepsilon_m \frac{(n-m)!}{(n+m)!} \cos(m(\phi - \bar{\phi})) \\ \quad \times P_n^m(\cos \theta) P_n^m(\cos \bar{\theta}) j'_n(k\bar{\rho}) h_n^{(2)}(k\bar{\rho}), & \bar{\rho} > \rho, \\ L^e(s, x) = ik^2 \sum_{n=0}^{\infty} (2n+1) \sum_{m=0}^n \varepsilon_m \frac{(n-m)!}{(n+m)!} \cos(m(\phi - \bar{\phi})) \\ \quad \times P_n^m(\cos \theta) P_n^m(\cos \bar{\theta}) j_n(k\bar{\rho}) h_n^{(2)}(k\bar{\rho}), & \rho > \bar{\rho}. \end{cases}$	$M(s, x) = \begin{cases} M^i(s, x) = ik^3 \sum_{n=0}^{\infty} (2n+1) \sum_{m=0}^n \varepsilon_m \frac{(n-m)!}{(n+m)!} \cos(m(\phi - \bar{\phi})) \\ \quad \times P_n^m(\cos \theta) P_n^m(\cos \bar{\theta}) j'_n(k\bar{\rho}) h_n^{(2)}(k\bar{\rho}), & \bar{\rho} \geq \rho, \\ M^e(s, x) = ik^3 \sum_{n=0}^{\infty} (2n+1) \sum_{m=0}^n \varepsilon_m \frac{(n-m)!}{(n+m)!} \cos(m(\phi - \bar{\phi})) \\ \quad \times P_n^m(\cos \theta) P_n^m(\cos \bar{\theta}) j'_n(k\bar{\rho}) h_n^{(2)}(k\bar{\rho}), & \rho > \bar{\rho}. \end{cases}$
Orthogonal process	$\begin{aligned} & \int_0^{2\pi} \int_0^\pi ik^2 \sum_{n=0}^{\infty} (2n+1) \sum_{m=0}^n \varepsilon_m \frac{(n-m)!}{(n+m)!} \cos(m(\phi - \bar{\phi})) \\ & \quad \times P_n^m(\cos \theta) P_n^m(\cos \bar{\theta}) j'_n(k\bar{\rho}) h_n^{(2)}(k\bar{\rho}) \\ & \quad \times P_n^m(\cos \bar{\theta}) \cos(m\bar{\phi}) \bar{\rho}^2 \sin(m\bar{\theta}) d\bar{\theta} d\bar{\phi} \\ & = 4\pi k^2 i \bar{\rho}^2 j'_n(k\bar{\rho}) h_n^{(2)}(k\bar{\rho}) P_n^m(\cos \theta) \cos(m\phi), \quad \bar{\rho} > \rho, \\ & \int_0^{2\pi} \int_0^\pi ik^2 \sum_{n=0}^{\infty} (2n+1) \sum_{m=0}^n \varepsilon_m \frac{(n-m)!}{(n+m)!} \cos(m(\phi - \bar{\phi})) \\ & \quad \times P_n^m(\cos \theta) P_n^m(\cos \bar{\theta}) j_n(k\bar{\rho}) h_n^{(2)}(k\bar{\rho}) \\ & \quad \times P_n^m(\cos \bar{\theta}) \cos(m\bar{\phi}) \bar{\rho}^2 \sin(m\bar{\theta}) d\bar{\theta} d\bar{\phi} \\ & = 4\pi k^2 i \bar{\rho}^2 j'_n(k\bar{\rho}) h_n^{(2)}(k\bar{\rho}) P_n^m(\cos \theta) \cos(m\phi), \quad \bar{\rho} < \rho. \end{aligned}$	$\begin{aligned} & \int_0^{2\pi} \int_0^\pi ik^3 \sum_{n=0}^{\infty} (2n+1) \sum_{m=0}^n \varepsilon_m \frac{(n-m)!}{(n+m)!} \cos(m(\phi - \bar{\phi})) \\ & \quad \times P_n^m(\cos \theta) P_n^m(\cos \bar{\theta}) j'_n(k\bar{\rho}) h_n^{(2)}(k\bar{\rho}) \\ & \quad \times P_n^m(\cos \bar{\theta}) \cos(m\bar{\phi}) \bar{\rho}^2 \sin(m\bar{\theta}) d\bar{\theta} d\bar{\phi} \\ & = 4\pi k^3 i \bar{\rho}^2 j_n(k\bar{\rho}) h_n^{(2)}(k\bar{\rho}) P_n^m(\cos \theta) \cos(m\phi), \quad \bar{\rho} \geq \rho, \\ & \int_0^{2\pi} \int_0^\pi ik^3 \sum_{n=0}^{\infty} (2n+1) \sum_{m=0}^n \varepsilon_m \frac{(n-m)!}{(n+m)!} \cos(m(\phi - \bar{\phi})) \\ & \quad \times P_n^m(\cos \theta) P_n^m(\cos \bar{\theta}) j'_n(k\bar{\rho}) h_n^{(2)}(k\bar{\rho}) \\ & \quad \times P_n^m(\cos \bar{\theta}) \cos(m\bar{\phi}) \bar{\rho}^2 \sin(m\bar{\theta}) d\bar{\theta} d\bar{\phi} \\ & = 4\pi k^3 i \bar{\rho}^2 j'_n(k\bar{\rho}) h_n^{(2)}(k\bar{\rho}) P_n^m(\cos \theta) \cos(m\phi), \quad \bar{\rho} < \rho. \end{aligned}$
Limit $\rho \rightarrow \bar{\rho}$	$\begin{cases} 4\pi k^2 i \bar{\rho}^2 j'_n(k\bar{\rho}) h_n^{(2)}(k\bar{\rho}) P_n^m(\cos \theta) \cos(m\phi), & \bar{\rho} > \rho, \\ 4\pi k^2 i \bar{\rho}^2 j_n(k\bar{\rho}) h_n^{(2)}(k\bar{\rho}) P_n^m(\cos \theta) \cos(m\phi), & \bar{\rho} < \rho. \end{cases} \text{(Jump for } \bar{\rho}^- < \rho < \bar{\rho}^+ \text{ is } 4\pi k \sum_{n=0}^{\infty} \sum_{m=0}^n P_n^m(\cos \theta) \cos(m\phi))$	$\begin{cases} 4\pi k^2 i \bar{\rho}^2 j_n(k\bar{\rho}) h_n^{(2)}(k\bar{\rho}) P_n^m(\cos \theta) \cos(m\phi), & \bar{\rho} \geq \rho, \\ 4\pi k^2 i \bar{\rho}^2 j'_n(k\bar{\rho}) h_n^{(2)}(k\bar{\rho}) P_n^m(\cos \theta) \cos(m\phi), & \bar{\rho} < \rho. \end{cases} \text{(Continuous for } \bar{\rho}^- < \rho < \bar{\rho}^+ \text{)}$

**References**

- 459      [1] Chen IL, Chen JT, Lee WM, Kao SK. Computer assisted proof of spurious  
460      eigensolution for annular and eccentric membranes. *J Mar Sci Technol*; in  
461      press.
- 462      [2] Ali A, Rajakumar C, Yunus SM. Advances in acoustic eigenvalue analysis using  
463      boundary element method. *Comput Struct* 1995;56(5):837–47.
- 464      [3] Winkler JR, Davies JB. Elimination of spurious modes in finite element analysis.  
465      *J Comput Phys* 1984;56:1–14.
- 466      [4] Greenberg MD. Advanced engineering mathematics. New Jersey: Prentice-  
467      Hall; 1998.
- 468      [5] Fujiwara H. High-accurate numerical computation with multiple-precision  
469      arithmetic and spectral method, unpublished report; 2007.
- 470      [6] Zhao S. On the spurious solutions in the high-order finite difference methods  
471      for eigenvalue problems. *Comput Methods Appl Mech Eng* 2007;196:5031–46.
- 472      [7] Kuo SR, Chen JT, X Huang C. Analytical study and numerical experiments for  
473      true and spurious eigensolutions of a circular cavity using the real-part dual  
474      BEM. *Int J Numer Methods Eng* 2000;48:1401–22.
- 475      [8] Chen JT, Wong FC. Analytical derivations for one-dimensional eigenproblems  
476      using dual boundary element method and multiple reciprocity method. *Eng Anal Bound Elem*  
477      1997;20:25–33.
- 478      [9] Chen JT, Wong FC. Dual formulation of multiple reciprocity method for the  
479      acoustic mode of a cavity with a thin partition. *J Sound Vib* 1998;217(1):  
480      75–95.
- 481      [10] Yeih W, Chen JT, Chen KH, Wong FC. A study on the multiple reciprocity  
482      method and complex-valued formulation for the Helmholtz equation. *Adv Eng  
483      Soft* 1998;29(1):1–6.
- 484      [11] Yeih W, Chen JT, Chang CM. Applications of dual MRM for determining the  
485      natural frequencies and natural modes of an Euler-Bernoulli beam using the  
486      singular value decomposition method. *Eng Anal Bound Elem* 1999;23:339–60.
- 487      [12] Yeih W, Chang JR, Chang CM, Chen JT. Applications of dual MRM for  
488      determining the natural frequencies and natural modes of a rod using the  
489      singular value decomposition method. *Adv Eng Soft* 1999;30:459–68.
- 490      [13] Chen JT, Kuo SR, Chung IL, Huang CX. Study on the true and spurious  
491      eigensolutions of two-dimensional cavities using the multiple reciprocity  
492      method. *Eng Anal Bound Elem* 2003;27:655–70.
- 493      [14] Chen JT, Lin JH, Kuo SR, Chyuan SW. Boundary element analysis for the  
494      Helmholtz eigenvalue problems with a multiply connected domain. *Proc Roy  
495      Soc A* 2001;457:2521–46.
- 496      [15] Chen JT, Liu LW, Hong HK. Spurious and true eigensolutions of Helmholtz BIEs  
497      and BEMs for a multiply-connected problem. *Proc Roy Soc A* 2003;459:1891–925.
- 498      [16] Chen JT, Chen IL, Chen KH. Treatment of rank deficiency in acoustics using SVD.  
499      *J Comput Acoust* 2006;14(2):157–83.
- 500      [17] Tsai CC, Young DL, Chen CW, Fan CN. The method of fundamental solutions for  
501      eigenproblems in the domains with and without interior holes. *Proc Roy Soc A*  
502      2006;462:1443–66.
- 503      [18] Chen JT, Lee CF, Lin SY. A new point of view for the polar decomposition using  
504      singular value decomposition. *Int J Comput Numer Anal* 2002;2(3):257–64.
- 505      [19] Chen JT, Shen WC, Wu AC. Null-field integral equations for stress field around  
506      circular holes under anti-plane shear. *Eng Anal Bound Elem*  
507      2006;30(3):205–17.
- 508      [20] Chen JT, Chen PY. A semi-analytical approach for stress concentration of  
509      cantilever beams with holes under bending. *J Mech* 2007;23(3):211–21.
- 510      [21] Chen JT, Chen CT, Chen PY, Chen IL. A semi-analytical approach for radiation  
511      and scattering problems with circular boundaries. *Comput Methods Appl  
512      Mech Eng* 2007;196:2751–64.
- 513      [22] Chen JT, Chen CT, Chen PY, Chen IL. A semi-analytical approach for radiation  
514      and scattering problems with circular boundaries. *Comput Methods Appl  
515      Mech Eng* 2007;196:2751–64.